Supporting Information

A (3,8)-connected metal-organic framework with a unique binuclear [$Ni_2(\mu_2$-OH)($COO)_2$] node for high H_2 and CO_2 adsorption capacities

Lei Zhang,[ab] Jinjie Qian,[a] Wenbin Yang,[a] Xiaofei Kuang,[a] Jun Zhang,[a] Yixin Cui,[a] Weiming Wu,[a] Xiao-Yuan Wu,[a] Can-Zhong Lu*[a] and Wen-Zhe Chen*[bc]

[a]*Key Laboratory of Design and Assembly of Functional Nanostructures, Fujian Institute of Research on the Structure of Matter, Chinese Academy of Sciences, Fuzhou, Fujian 350002, P. R. China.*

E-mail: czlu@fjirsm.ac.cn; Fax: (+86)591-83714946

[b]*College of Materials Science and Engineering, Fuzhou University, Fuzhou, Fujian 350116, P. R. China.*

E-mail: chenwz@fzu.edu.cn; Fax: (+86)591-22866538

[c]*Xiamen University of Technology, Xiamen, Fujian 361024, P. R. China.*

Experimental Section

General procedure

The ligand tris-(4-pyridyl)-1,3,5-triazine (tpt) was synthesized according to the literature method.[1] The other solvents and reagents were purchased from commercial sources and used without purification. Infrared (IR) spectra were recorded on a Vertex 70 using KBr pallets. Elemental analyses of (C, H and N) were carried out with a Vario EL III elemental analyzer. Thermogravimetric analysis (TGA) was performed with a TGA/DSC 1 STAR^e system at a heating rate of 5 ºC/min under nitrogen atmosphere. Powder X-ray diffraction (PXRD) measurements were carried out at room temperature on a Rigaku MiniFlex600 diffractometer using Cu *K*α radiation (λ = 0.154 nm). *In situ* variable temperature PXRD patterns were recorded on a Rigaku Ultima IV diffractometer. Single component gas adsorption measurements were collected in the Accelerated Surface Area and Porosimetry 2020 System (ASAP2020).

Synthesis procedure

Synthesis of $[Ni_2(\mu_2\text{-}OH)(bpdc)(tpt)_2][NO_3]\cdot 3DMA\cdot 4CH_3OH\cdot 6H_2O$ (1)

$Ni(NO_3)_2\cdot 6H_2O$ (0.034 g, 0.12 mmol), tpt (0.034 g, 0.11 mmol) and H_2bpdc (0.014 g, 0.06 mmol) were added in the solvent mixture of N,N-dimethylacetamide (DMA, 5 mL)/methanol (CH_3OH, 5 mL) solvent in a 20 mL screw-capped vial, then 100μL HBF_4 (Tetrafluoroboric acid, 40% in water) was added into the solution and the mixture was sonicated for 30 min. Finally, the mixture was sealed and heated to 85 °C for 5 days. The green block crystals of **1** were filtered and washed with DMA, then washed with ethanol three times and dried in the air. (Yield: 68.2% based on nickel). Elemental analysis: Calcd. (Found %) For $C_{66}H_{88}N_{16}Ni_2O_{21}$ **1**: C, 50.80 (50.61); H, 5.64 (5.74); N, 14.37 (14.22).

Crystallographic Study

Crystallographic data of **1** was collected on a Saturn 70 diffractometer equipped with graphite-monochromated Mo Kα radiation (λ=0.71073 Å) at 100 K. The CrystalClear program was used for the absorption correction. The structure was solved by direct methods and refined on F^2 by full-matrix, least-squares methods using the SHELXL-97 program package.[2] All non-hydrogen atoms were refined anisotropically. The hydrogen atoms for the ligands were placed in calculated positions and treated as riding on their parents, while the hydrogen atoms of the μ_2-OH hydroxyl groups were not included in the model. It should be noted here that there are many disordered charge-balancing NO_3^- counter anions lying inside the extra-large solvent accessible interspaces, which lead to the final charge equilibrium. One NO_3^- anion per formula unit was suggested by elemental analysis and thermogravimetric analysis. The contributions of disordered solvent molecules and the charge-balancing NO_3^- anions were treated as diffuse using the SQUEEZE procedure implemented in PLATON,[3] subsequently a set of solvent-free diffraction intensities was produced. The final formula of **1** was figured out based on the SQUEEZE results, elemental analysis data and TGA data. A summary of crystallographic refinement details for **1** were given in table S1. Complete details can be found in the accompanying cif file. The following crystal structure has been deposited at the Cambridge Crystallographic Data Centre and the CCDC number (1061092) is for **1**.

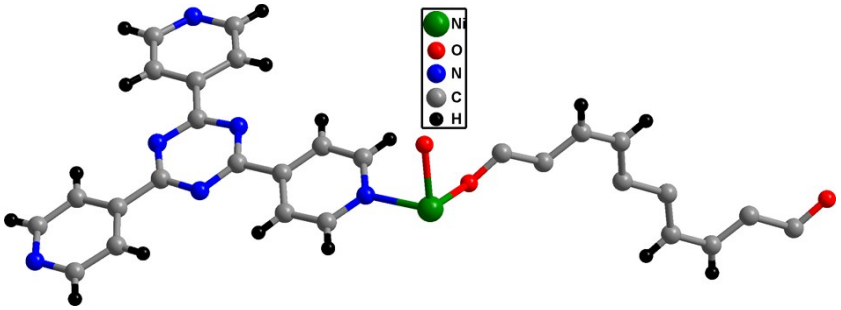

Fig. S1 The asymmetric unit of **1**.

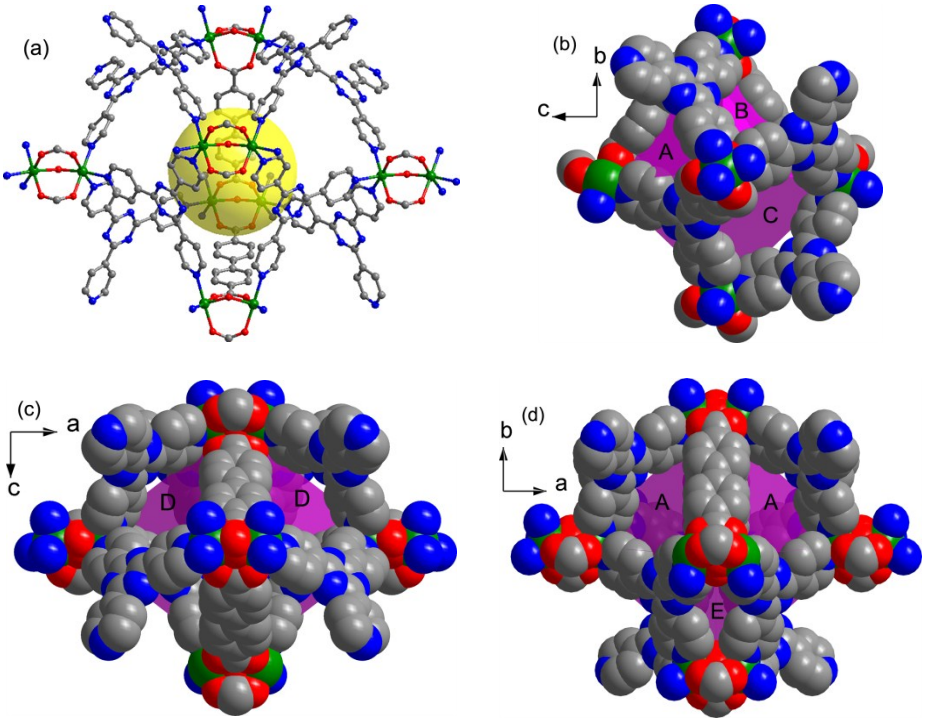

Fig. S2 (a) The irregular octahedral cage with a cavity diameter of about 6.0 Å. (b) Views of the irregular octahedral cage with three types of small windows (A: ~9.3 × 9.5 Å; B: ~8.1 × 8.2 Å and C: ~9.3 × 10.6 Å) along the *a* axis. (c) Views of the irregular octahedral cage with a small windows (D: ~9.6× 9.7 Å) along the *b* axis. (c) Views of the irregular octahedral cage with two kinds of small windows (E: ~6.5× 8.2 Å and A: ~9.3 × 9.5 Å) along the *c* axis.

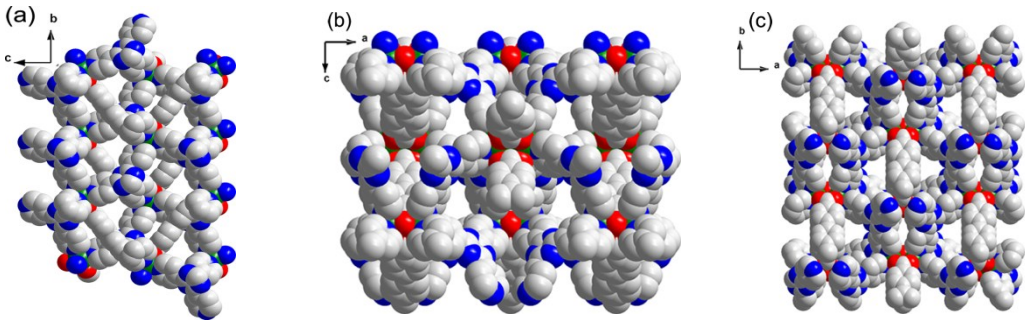

Fig. S3 Views of the 3D framework of **1** along three crystallographic axes.

Table S1 Summary of Crystal Data and Structure Refinement for **1**.

	1
Empirical formula	$C_{66}H_{88}N_{16}Ni_2O_{21}$
Formula weight	1558.94
Temperature	153 (2) K
Wavelength	0.71073 Å
Crystal system, space group	Orthorhombic, $Cmc2_1$
Unit cell dimensions	a = 24.345 (4) Å α = 90°
	b = 20.477 (3) Å β = 90°
	c = 19.098 (3) Å γ = 90°
Volume	9521 (3) $Å^3$
Z	4
Density (calculated)	1.067 g/cm^3
Absorption coefficient	0.460 mm^{-1}
F (000)	3224
Crystal size	0.25× 0.25 × 0.20 mm
Theta range for data collection	2.26° to 27.50°
Index ranges	-28 <= h <= 31
	-24 <= k <= 25
	-24 <= l <= 24
Reflections collected / unique	29797 / 10913 [R(int) = 0.0168]
Absorption correction	Multi-scan
Refinement method	Full-matrix least-squares on F^2
Data / restraints / parameters	10913 / 1 / 321
Goodness-of-fit on F^2	1.062
Final R indices [I>2sigma(I)]	R_1 = 0.0298, wR_2 = 0.0828
R indices (all data)	R_1 = 0.0307, wR_2 = 0.0836
Largest diff. peak and hole	0.530 and -0.345 $e·Å^{-3}$

Physical Measurements

Infrared measurements

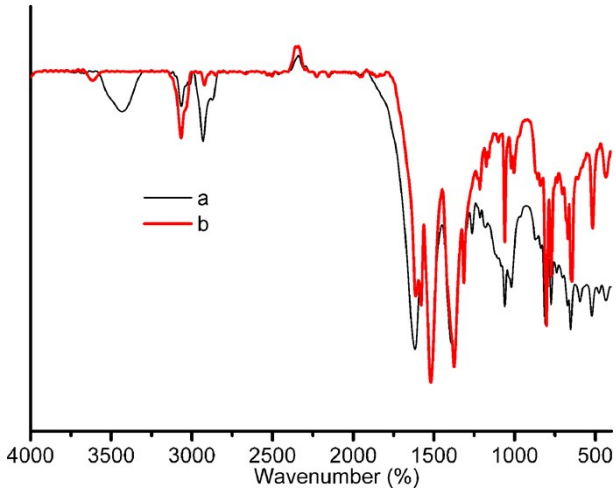

Fig. S4 The IR spectra of **1** recorded at room temperature under room atmosphere (a) and after losing of solvent water molecules during 2 h under vacuum at 200 °C (b). The IR peak of the μ_2-OH hydroxyl group of **1** is at 3612 cm^{-1} after the loss of solvent water molecules (b), and the ν(OH) mode is shifted to 3430 cm^{-1} when the hydroxyl group is involved in hydrogen bond interaction with the trapped water molecules (a).[4]

Thermogravimetric analysis

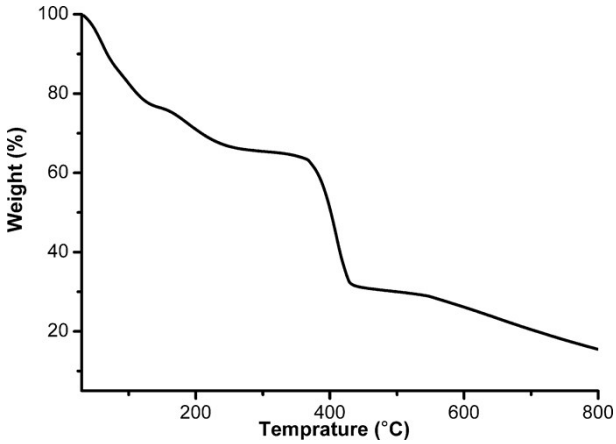

Fig. S5 TGA curve of **1**.

Powder X-ray diffraction

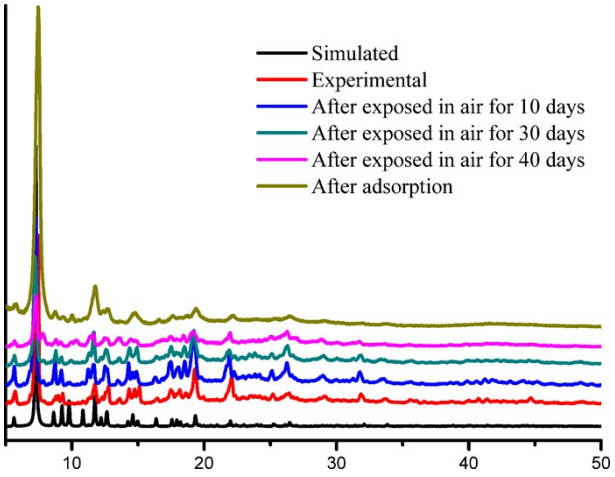

Fig. S6 The PXRD patterns of **1** obtained in different conditions.

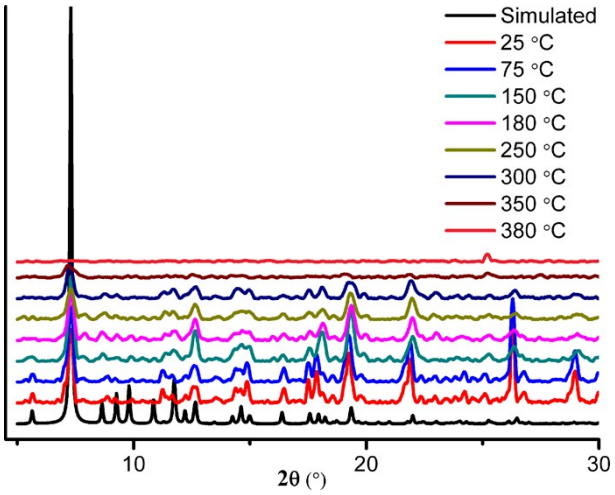

Fig. S7 *In situ* variable temperature PXRD patterns for **1** under room atmosphere.

Gas adsorption measurements

A Micromeritics (Accelerated Surface Area and Porosimetry) 2020 System was used to measure gas adsorption. In order to remove the nonvolatile solvates, the fresh samples of **1** were soaked in acetone for 3 days and the soaking solution was replaced by fresh acetone every 12 hours, and then degassed under dynamic vacuum at 100 °C for 10 hours to obtain the completely activated samples **1a**. The N_2 and H_2 gas

adsorption isotherms were measured at 77 K or 87 K using a liquid N_2 or Ar bath, respectively. In addition, the CO_2, CH_4 and N_2 adsorption isotherms were measured at 273 K, 283 K and 295 K, and the temperature was held constant using an ice water bath or water bath.

Isosteric heats of adsorption (Q_{st})

The isosteric heats of adsorption (Q_{st}) for H_2 and CO_2 was fitted by a virial method **(1)**[5] using the H_2 adsorption isotherms (77 K and 87 K) and the CO_2 isotherms (273, 283 and 295 K), respectively, and then calculated by using the Clausius-Clapeyron equation **(2)**.

$$\ln P = \ln N + 1/T \sum_{i=0}^{m} a_i N^i + \sum_{j=0}^{n} b_j N^j \quad \textbf{(1)}$$

$$Q_{st} = -R \sum_{i=0}^{m} a_i N^i \quad \textbf{(2)}$$

Where P is pressure (mmHg), N is the amount adsorbed quantity (mmol g^{-1}), T is the temperature (K), a_i and b_i are virial coefficients, R is the real gas constant, and m, n represent the number of coefficients required to adequately describe the isotherms.

Prediction of the gases adsorption selectivity by IAST

IAST (ideal adsorption solution theory)[6] was used to predict binary mixture adsorption from the experimental pure-gas isotherms. For CO_2, CH_4 and N_2 isotherms of **1a** in the low pressure, the experimental isotherm data (measured at 273 and 295 K) were fitted using the single-site Langmuir-Freundlich equation **(3)**.

$$q = \frac{q_{sat} b p^c}{1 + b p^c} \quad \textbf{(3)}$$

Where, b is the parameter in the pure component Langmuir isotherm (kPa^{-1}), p is bulk gas phase pressure of species (kPa), q is the adsorbed amount of adsorbent (mmol g^{-1}),

q_{sat} is saturation capacity of species (mmol g^{-1}), c is constant.

The adsorption selectivities (S_{ads}) for binary mixtures of CO_2/CH_4 and CO_2/N_2, defined by

$$S_{ads} = \frac{x_1 / x_2}{y_1 / y_2} \quad \textbf{(4)}$$

Where x_i is the mole fractions of component i in the adsorbed phases and y_i is the mole fractions of component i in the bulk phases.

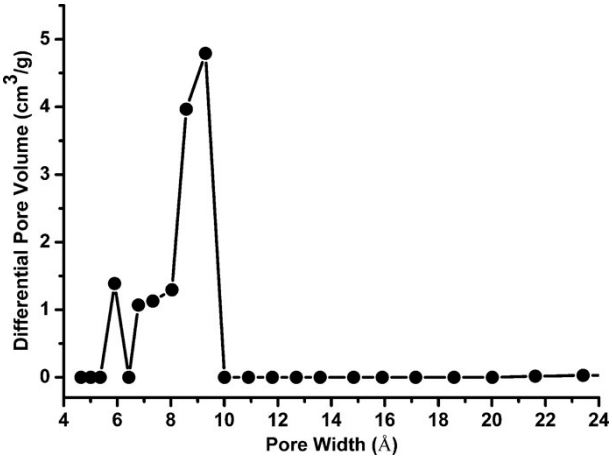

Fig. S8 The pore size distribution of **1a** calculated by density functional theory method.

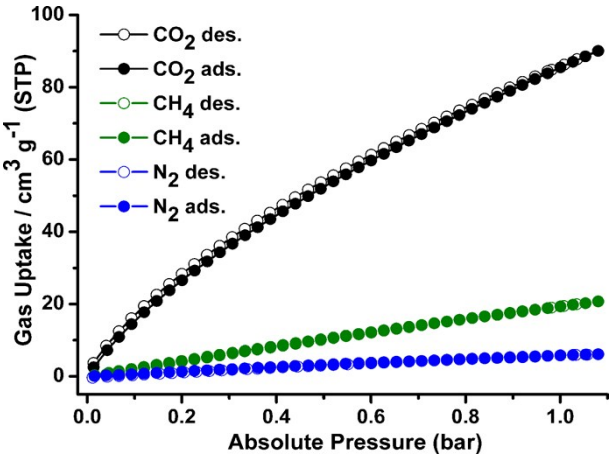

Fig. S9 CO_2, CH_4 and N_2 adsorption isotherms of **1a** at 283 K.

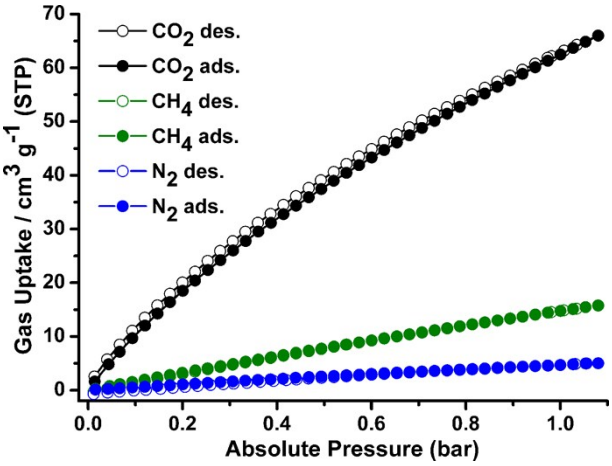

Fig. S10 CO_2, CH_4 and N_2 adsorption isotherms of **1a** at 295 K.

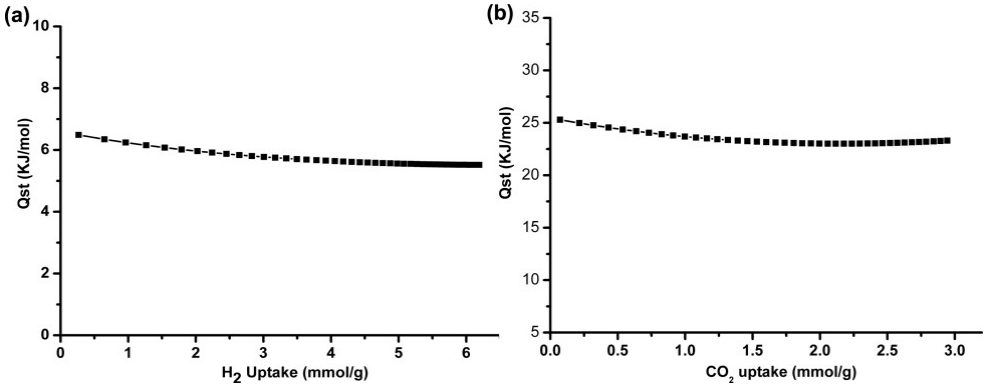

Fig. S11 The isosteric heats of adsorption (Q_{st}) of H_2 (a) and CO_2 (b) calculated by the virial method for **1a**.

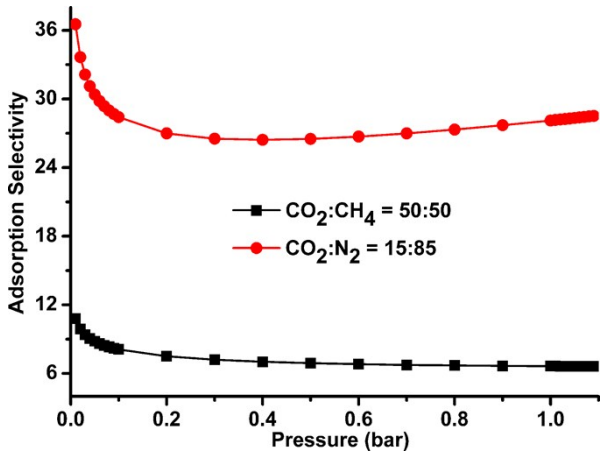

Fig. S12 IAST calculations of CO_2/CH_4 and CO_2/N_2 adsorption selectivities for **1a** at 295 K.

Additional Figures and Descriptions

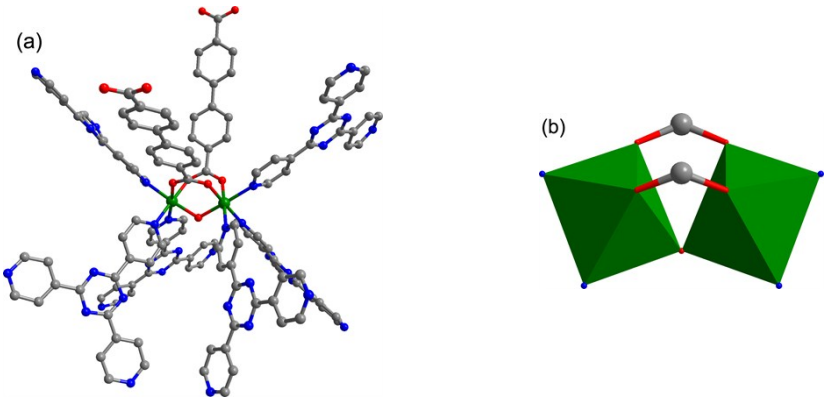

Fig. S13 **(**a) The coordination environment of the binuclear [$Ni_2(\mu_2$-OH)$(COO)_2$] node. (b) A pair of adjacent Ni(II) octahedral with sharing a bridging μ_2-OH hydroxyl group.

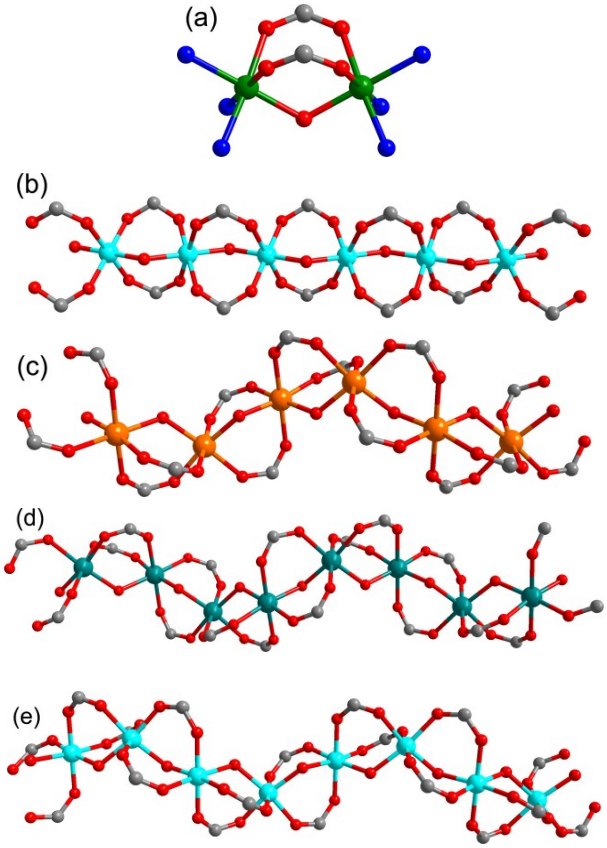

Fig. S14 The binuclear [$Ni_2(\mu_2$-OH)$(COO)_2$] SBU in **1** (a). View of the infinite 1-periodic binuclear [$M_2(\mu_2$-OH)($COO)_2$] SBUs in MIL-53 (b), NOTT-400 (c), InOF-1 (d), NOTT-300 (e).[7] (C, gray; N, blue; O, red; Ni, green; Al, turquoise; Sc, orange; In, teal).

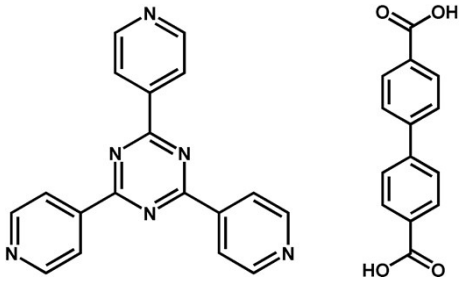

Fig. S15 Structures of the organic ligands tpt and H_2bpdc.

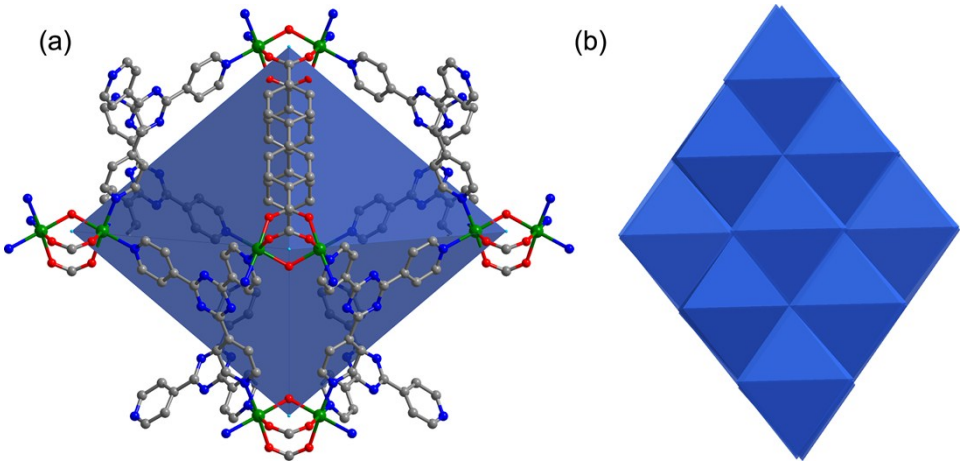

Fig. S16 (a) Six $[Ni_2(\mu_2\text{-}OH)(COO)_2]$ SBUs are bonded together by two $bpdc^{2-}$ ligands and eight tpt ligands to form an irregular octahedral cage in **1**. (b) View of the ABAB octahedral cage packing in the 3D framework of **1**.

Bond valence sum (BVS) analysis for 1

The bond-valence model based on the Brown equation **(5)**[8] was applied to assess the oxidation state of the nickel ions and bridging oxygen atoms in **1**, and the results of the calculations are shown in Table S2.

$$V_i = \sum_j V_{ij} = \sum_j \exp\left(\frac{r_o - r_{ij}}{B}\right) \quad \textbf{(5)}$$

Where V_i is the atom valence of a given atom, i, which is equal to the sum of all bond valences of the bonds formed by the given atom, i. V_{ij} is the valence of a bond between two atoms, i and j. r_0 is an empirical parameter determined for pairs of atoms. r_{ij} is the bond length between atoms i and j. In this work, i and j are Ni and O or Ni and N. B is a constant, the "universal parameter" ~0.370 Å.

Table S2 BVS Calculation for **1.**

Ni^{2+}	r_0	r_{ij}	B	V_{ij}
Ni1—O1	1.670	1.9797 (6)	0.370	0.433
Ni1—O3^{i}	1.670	2.0392 (9)	0.370	0.369
Ni1—O2	1.670	2.0501 (11)	0.370	0.358
Ni1—N1	1.647	2.0918 (12)	0.370	0.301
Ni1—N3^{ii}	1.647	2.1076 (11)	0.370	0.288
Ni1—N2^{iii}	1.647	2.1337 (13)	0.370	0.268
$V_{Ni} = \Sigma V_{ij} = 2.017$; $V_{O1} = 2 \times V_{Ni1\text{-}O1} = 0.866$				
Ni^{3+}	r_0	r_{ij}	B	V_{ij}
Ni1—O1	1.750	1.9797 (6)	0.370	0.538
Ni1—O3^{i}	1.750	2.0392 (9)	0.370	0.458
Ni1—O2	1.750	2.0501 (11)	0.370	0.444
Ni1—N1	1.731	2.0918 (12)	0.370	0.377
Ni1—N3^{ii}	1.731	2.1076 (11)	0.370	0.361
Ni1—N2^{iii}	1.731	2.1337 (13)	0.370	0.337
$V_{Ni} = \Sigma V_{ij} = 2.515$; $V_{O1} = 2 \times V_{Ni1\text{-}O1} = 1.076$				

Symmetry codes: (i) -*x*, -*y*-1, *z*-1/2; (ii) *x*, -*y*, *z*+1/2; (iii) -*x*+1/2, -*y*-1/2, *z*+1/2.

Table S3 Selected Bond Lengths (Å) and Angles (º) for **1**.

Bond	Distance (Å)	O3^{i}—Ni1—N1	86.93 (5)
Ni1—O1	1.9797 (6)	O2—Ni1—N1	179.56 (5)
Ni1—O3^{i}	2.0392 (9)	O1—Ni1—N3^{ii}	87.30 (4)

Ni1—O2	2.0501 (11)	$O3^{i}$—Ni1—$N3^{ii}$	174.91 (4)
Ni1—N1	2.0918 (12)	O2—Ni1—$N3^{ii}$	91.49 (4)
Ni1—$N3^{ii}$	2.1076 (11)	N1—Ni1—$N3^{ii}$	88.95 (5)
Ni1—$N2^{iii}$	2.1337 (13)	O1—Ni1—$N2^{iii}$	173.30 (5)
Angle	(º)	$O3^{i}$—Ni1—$N2^{iii}$	87.61 (4)
O1—Ni1—$O3^{i}$	95.55 (4)	O2—Ni1—$N2^{iii}$	82.15 (5)
O1—Ni1—O2	91.79 (4)	N1—Ni1—$N2^{iii}$	97.86 (5)
$O3^{i}$—Ni1—O2	92.63 (4)	$N3^{ii}$—Ni1—$N2^{iii}$	90.01 (4)
O1—Ni1—N1	88.22 (4)	Ni1—O1—$Ni1^{iv}$	119.61 (5)

Symmetry codes: (i) -*x*, -*y*-1, *z*-1/2; (ii) *x*, -*y*, *z*+1/2; (iii) -*x*+1/2, -*y*-1/2, *z*+1/2; (iv) -*x*, *y*, *z*.

Table S4 Comparison of H_2 Adsorption Capacities in Selected Metal-organic Frameworks at 77 K and 1.0 Bar.

Material	Surface Area (m^2/g)		Pore Volume	H_2 Uptake	H_2 Q_{st}	Ref.
	BET	Langmuir	cm^3/g	wt%	kJ/mol	
1a	1489	1680	0.62	1.81	6.5	This work
NOTT-400	1350		0.56	2.14	5.96	7b
NOTT-401	1514		0.66	2.31	6.65	7b
FJI-2	1177	1355	0.48	1.34	7.2	9
ZIF-8	1630	1810	0.64	1.27		10
SNU-6	2590	2910	1.05	1.68	7.74	11
IRMOF-6	2476	3263	1.14	1.48		12

PCN-66	4000	4600	1.63	1.79	6.22	13

Table S5 Comparison of CO_2 (273-298 K) Adsorption Capacities in Selected Metal-organic Frameworks at 1.0 Bar.

Material	Surface Area (m^2/g)		Pore Volume	CO_2 Uptake	CO_2 Q_{st}	Ref.
	BET	Langmuir	cm^3/g	wt%, T	kJ/mol	
1a	1489	1680	0.62	21.3, 273 K 12.3, 295 K	25.3	This work
NJU-Bai3	2690	3100	1.08	21.4, 273 K	36.5	14
PCN-80	3850	3584	1.47	19.3, 273 K 12.0, 296 K	20.4	15
CAU-1	1268		0.61	24.1, 273 K	48	16
Cu-BTTri	1770	1900	0.713	14.3, 298 K	21	17
NOTT-140a	2620		1.07	11.7, 293 K	24.7	18

Table S6 Comparison of H_2 and CO_2 Adsorption Capacities of Metal-organic Frameworks with $[M_2(\mu_2\text{-}OH)(COO)_2]$ SBUs.

Material	Surface Area (m^2/g)		Pore Volume	P/T/Adsorption Capacity (H_2/CO_2)	Ref.
	BET	Langmuir	cm^3/g	bar /K/wt%	
1a	1489	1680	0.62	1/77/1.81 (H_2) 1/273/21.3 (CO_2)	This work
MIL-53(Al)	1100			16/77/3.8 (H_2)	19
NOTT-400	1350		0.56	1/77/2.14 (H_2)	7b
NOTT-401	1514		0.66	1/77/2.31 (H_2)	7b

InOF-1	1065	1093	0.37	1/273/27.5 (CO_2)	7c
NOTT-300			0.375	1/273/30.8 (CO_2)	7d

References

1. M. X. Li, Z. X. Miao, M. Shao, S. W. Liang and S. R. Zhu, *Inorg. Chem.*,2008, **47**, 4481.
2. G. M. Sheldrick, *Acta. Crystallogr.*,2008, **A64**, 112.
3. A. L. Spek, *J. Appl. Crystallogr.*, 2003, **36**, 7; P. v. d. Sluis and A. L. Spek, *Acta Crystallogr*., *Sect. A,* 1990, **46**, 194.
4. A. Vimont, A. Travert, P. Bazin, J.-C. Lavalley, M. Daturi, C. Serre, G. Ferey, S. Bourrelly and P. L. Llewellyn, *Chem. Commun.*, 2007, 3291-3293.
5. J. L. Rowsell and O. M. Yaghi, *J. Am. Chem. Soc.*, 2006, **128**, 1304.
6. A. L. Myers, J. M. Prausnitz, *AIChE J.*,1965, **11**, 121.
7. (a) T. Loiseau, C. Serre, C. Huguenard, G. Fink, F. Taulelle, M. Henry, T. Bataille and G. Férey, *Chem. Eur. J.*, 2004, **10**, 1373; (b) I. A. Ibarra, S. Yang, X. Lin, A. J. Blake, P. J. Rizkallah, H. Nowell, D. R. Allan, N. R. Champness, P. Hubberstey and M. Schröder, *Chem. Commun.*, 2011, **47**, 8304; (c) J. Qian, F. Jiang, D. Yuan, M. Wu, S. Zhang, L. Zhang and M. Hong, *Chem. Commun.*, 2012, **48**, 9696; (d) S. Yang, J. Sun, A. J. Ramirez-Cuesta, S. K. Callear, W. I. David, D. P. Anderson, R. Newby, A. J. Blake, J. E. Parker, C. C. Tang and M. Schroder, *Nat. Chem.*, 2012, **4**, 887.
8. I. D. Brown and D. Altermatt, *Acta Cryst. B*, 1985, **41**, 244.
9. J. Qian, F. Jiang, K. Su, J. Pan, L. Zhang, X. Li, D. Yuan and M. Hong, *J. Mater. Chem. A*, 2013, **1**, 10631.
10. K. S. Park, Z. Ni, A. P. Cote, J. Y. Choi, R. Huang, F. J. Uribe-Romo, H. K. Chae, M. O'Keeffe and O. M. Yaghi, *Proc. Natl. Acad. Sci. U.S.A.* 2006, **103**, 10186.
11. H. J. Park and M. P. Suh, *Chem. Eur. J.*, 2008, **14**, 8812.
12. J. L. C. Rowsell and O. M. Yaghi, *J. Am. Chem. Soc.*, 2006, **128**, 1304.

13. D. Q. Yuan, D. Zhao, D. F. Sun and H. C. Zhou, *Angew. Chem., Int. Ed.*, 2010, **49**, 5357.

14. J. Duan, Z. Yang, J. Bai, B. Zheng, Y. Li and S. Li, *Chem. Commun.*, 2012, **48**, 3058.

15. W. Lu, D. Yuan, T. A. Makal, J. R. Li and H. C. Zhou, *Angew. Chem., Int. Ed.*, 2012, **51**, 1580.

16. X. Si, C. Jiao, F. Li, J. Zhang, S. Wang, S. Liu, Z. Li, L. Sun, F. Xu, Z. Gabelica and C. Schick, *Energy Environ. Sci.*, 2011, **4**, 4522.

17. A. Demessence, D. M. D'Alessandro, M. L. Foo, J. R. Long, *J. Am. Chem. Soc.,* 2009, **131**, 8784.

18. C. Tan, S. Yang, N. R. Champness, X. Lin, A. J. Blake, W. Lewis and M. Schröder, *Chem. Commun.*, 2011, **47**, 4487.

19. G. Férey, M. Latroche, C. Serre, F. Millange, T. Loiseau and A. Percheron-Guegan, *Chem. Commun.*, 2003, **24**, 2976.